Available online at www.sciencedirect.com

ScienceDirect

Procedia Structural Integrity 18 (2019) 93–100

Structural Integrity Procedia

www.elsevier.com/locate/procedia

25th International Conference on Fracture and Structural Integrity

Effect of Porosity and Cell Topology on Elastic-Plastic Behavior of Cellular Structures

S.Raghavendra[a]*, A.Molinari[a], V.Fontanari[a], V.Luchin[b], G.Zappini[b], M.Benedetti[a],

[a]*Department of Industrial Engineering,University of Trento,Trento 38123,Italy*
[b]*Eurocoating Spa, Pergine Valsugana, Trento 38057, Italy*

Abstract

In this work we study the mechanical behavior of Ti6Al4V cellular structures by varying the randomness in the cell topology from regular cubic to completely random and the porosity of the structure. The porosity of the structure is altered by changing the strut thickness and the pore size to obtain a stiffness value between 0.5-12Gpa. The geometrical deviation in the structures from the as-designed values is studied by morphological characterization. The samples are subjected to compression and tensile loading to obtain the stiffness and the elastic-plastic behavior of the samples. Finite element modelling (FEM) is carried out on the as-designed structures for both tensile and compressive loading to study the effect of deviation between the as-designed and as-built structures. FEM is also carried out for as-built regular structures, by introducing the geometrical deviation to match the porosity of the as-built structures. Comparison of FEM and experimental results indicated that the effect of cell topology depends on the porosity values. Simulation results of as-built structures demonstrated the importance of defects in the structure.

Peer-review under responsibility of the Gruppo Italiano Frattura (IGF) ExCo.

Keywords: Cell topology, porosity, stress-strain, FEM

1.Introduction

Cellular lattice structures have found applications in various industries such as automobile, aerospace and medicine where structural optimization is required. They play a key role in reducing the weight of the structure without

* Corresponding author. Tel.: +39-348-381-7779; fax: +0-000-000-0000 .
E-mail address: sunil.raghavendra@unitn.it

2452-3216
Peer-review under responsibility of the Gruppo Italiano Frattura (IGF) ExCo.
10.1016/j.prostr.2019.08.143

compromising the required mechanical properties, they can be used to produce tailored components according to the loading conditions. Additive manufacturing technologies, such as selective laser melting (SLM) and electron beam melting (EBM) have influenced the development of various types of cellular structures based on unit cell models with complex geometries such as gyroid, diamond, octate, truncated octahedron (Bobbert et al., 2017). The effect of cell parameters such as cell wall thickness, pore diameters, strut curvature play a major role on the properties by varying the overall porosity of the structures. For biomedical applications, titanium alloys are considered due to their high strength to weight ratio and corrosion resistance properties. Porous structures for bio medical applications should possess the mechanical properties similar to the bone (Taniguchi et al., 2016) to avoid stress shielding phenomenon. Behavior of these implants under compression and fatigue load is of utmost importance, but to generalize the application of cellular materials it is also necessary to study their behavior under tensile loading. One other criterion that is of concern in AM structures is the geometrical discrepancy between the as-designed and the as-built structures. Studies have been carried out to explore the effect of process parameters such as direction of printing and laser strength on the build quality of the specimens (Qiu et al., 2015). Finite element analysis of the structures is often necessary to understand their mechanical behavior avoiding expensive trial-and-error experiments (Cuadrado et al., 2017).

In this study we focus on the elastic-plastic behavior in tensile and compressive loading of three types of cellular structures by varying the degree of randomness from completely regular to completely random structure. Along with the experimental results of the as-built structures, finite element (FEM) simulations are performed on the as-designed structures to emphasize the discrepancies between the two. The study also focuses on the combined effect of porosity and the cell topology on the mechanical properties.

2. Materials and methods

This section mainly focuses on the material used, specimen details, experimental and FE methodology considered in the study.

2.1 Specimen details

Specimens are manufactured using a Renishaw AM250 SLM machine. Titanium alloy (Ti6Al4V) powders are used for the SLM process. Three different topologies, regular cubic, irregular cubic and completely random structures are studied under three different porosity values are as shown in Fig,1(b),1(c),1(d) and described in the previous work (Raghavendra et al., 2018). The specimens are identified based with the cell wall thickness and pore size as shown in Fig.1. The specimen details are as described in table 1. 0720 batch of samples had the lowest porosity followed by 1550 and 1520. Porosity details are as explained in the previous work (Raghavendra et al., 2018)

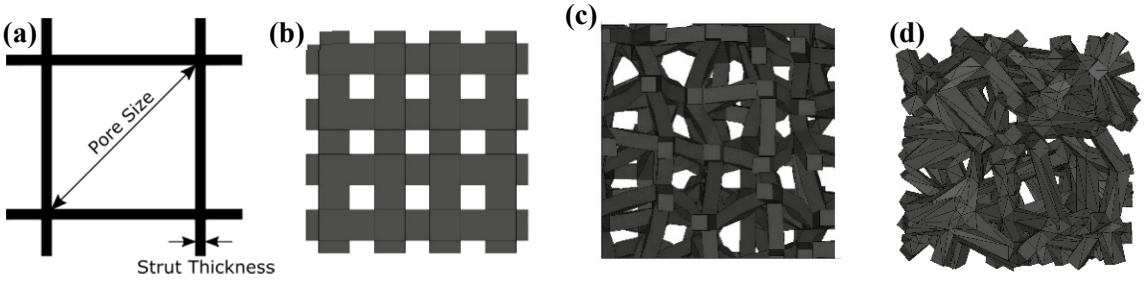

Fig.1. (a) Description of pore size and thickness (b) Regular structure (c) Irregular structure (d) Random structure

Table 1. Pore size and strut thickness of different batches (nominal values, from CAD files)

Sample	Pore Size (μm)	Strut thickness(μm)
1550	1500	500
0720	700	200
1520	1500	200

2.2 Porosity and Morphology

The porosity of the samples was calculated by the relative density method. The cellular specimens were cleaned and subjected to ultrasound cleaning. Later the specimens were weighed in a gravimetric weighing scale with a precision of 0.0001g. The volume of the specimen was calculated by measuring the height and diameter values at various locations. Porosity values were calculated using equation 1, where ρ is the density of the specimen and ρ_o is the density of the titanium alloy Ti-6Al-4V alloy (4.42g/cm3).

$$Porosity = \frac{\rho_o - \rho}{\rho_o} \quad (1)$$

The difference between the as-designed and the as-built structures are characterized by the morphological analysis. Two important parameters are considered for the analysis, strut thickness and the pore size, pore size is compared with the minimum feret diameter of the pores for comparison. JEOL JSM-IT300LV scanning electron microscope (SEM) is used for the strut thickness measurements, and Nikon stereomicroscope is used to measure the minimum feret diameter (minimum distance between the parallel tangents of the circumference of the pore).

2.3 Tensile and compression test

The mechanical characterization was carried out using monotonic tensile and compression test at room temperature for three specimens in each configuration. Both the tensile and compression test (ISO 13314:2011, ISO Standards,2011) were conducted on an Instron universal testing machine at a constant cross head speed of 1mm/min and a sampling rate of 1kHz. The displacement in compression and tensile test is measured using a LVDT and 12.5mm Instron extensometer. Data acquisition was carried out using a series IX and SAX V9.3 softwares.

The elastic modulus of the specimens is calculated on 0.2% strain line parallel to the elastic region of the stress strain curve. The strength of the material in tensile and compression loading is calculated by ultimate tensile strength and offset compressive strength. Ultimate tensile strength is obtained directly from the stress-strain curve while offset compressive strength is obtained along a 4% offset line from 0.2% strain line.

2.4 Finite element analysis

Due to the variation in the as-designed and as-built structures, finite element analysis of the as-designed structures was carried out in both compressive and tensile loading conditions. A mesh convergence study was carried out for all the batches of specimen. The STL files are converted into volume using Autodesk Inventor, the CAD files are meshed using 10 noded tetrahedron elements (SOLID187) in HYPERMESH V12. Analysis and the post processing of the results are carried out using ANSYS V16. A multilinear material model is considered from the tensile test data of the specimen produced from SLM, with a Young's modulus of 109 GPa. Initially, a mesh convergence study is carried out for all the batches of specimens due to the variation in strut thickness values. For regular structures as FE model of 5x5x5 unit cells were considered (Yang, 2016), for the irregular and random structures 5x5x5mm cube is considered for the analysis. To simulate the testing conditions, the bottom face of the sample is completely fixed while the top face of the sample is subjected to tensile and compressive loads. Displacement loads are applied to reduce the computation time (Helou et al., 2016)

Since it is not easy to replicate the as-designed structure into a FE model. Only regular cell topology was replicated based on the average thickness values and the measured porosity, regular cubic structures are developed using by

increasing the strut thickness by ~200µm. Defects from the SLM process such as strut waviness, missing struts and eccentricity of the junctions are not considered to reduce the complexity. These defects have a considerable effect on the elastic properties (Dallago et al., 2019). Tensile loading is carried out as discussed before, for compression testing a study was performed by giving an initial horizontal displacement along with compression load.

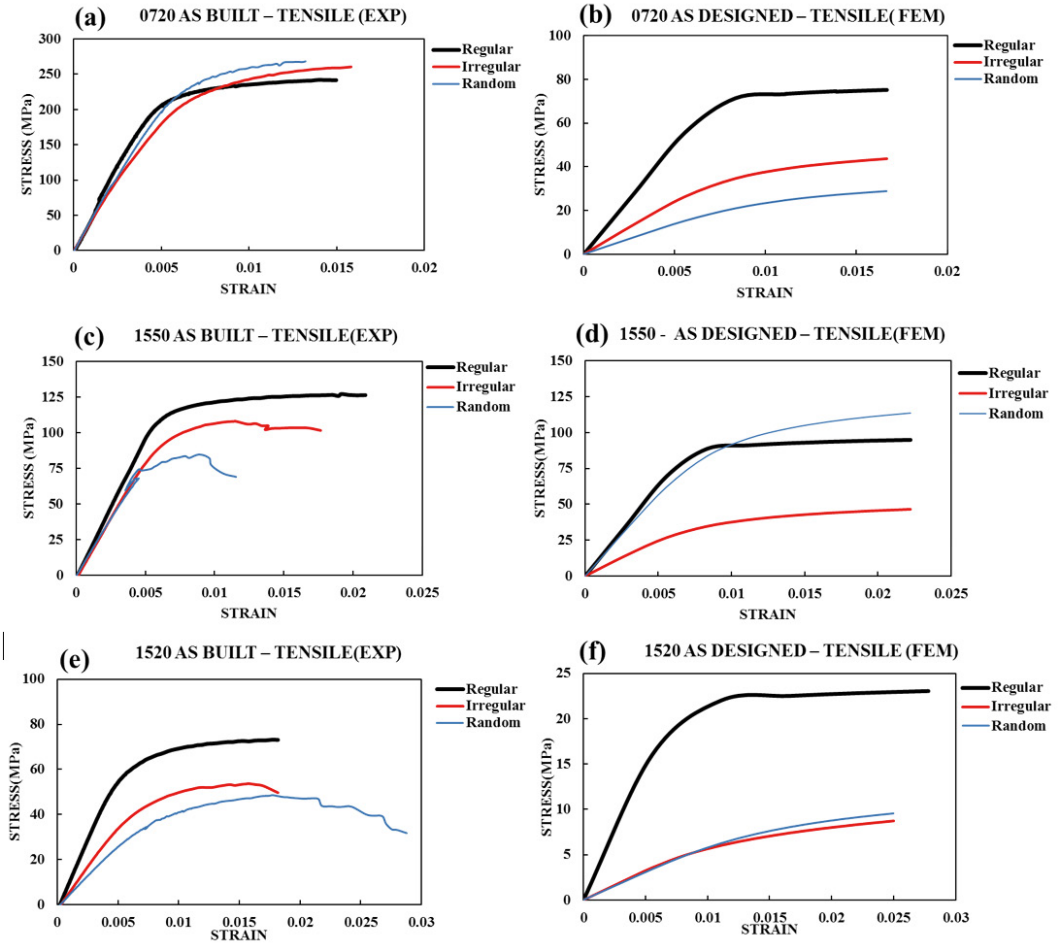

Fig. 2. Tensile stress-strain curves in experimental and FEM: (a) and (b) 0720, (c) and (d)1550, (e) and (f) 1520

3. Results and discussion

3.1 Porosity and Morphology

As mentioned in the previous work, (Raghavendra et.al.,2018) a difference in porosity of the as-built and as-designed structures is seen. The designed porosity of 0720,1550 and 1520 are in the range of 80%, 75% and 95% while the porosity values of as-designed structures are 45%,58% and 76% respectively. A maximum error of 50% was observed for 0720 samples with regular structures. Morphological analysis of the samples indicated an increase in the strut thickness values by an average of 220-250µm. This explains the proportional decrease in the porosity and the pore size (minimum feret diameter) of the samples. It is seen that minimum deviation is observed in vertical struts.

The geometrical deviations of the as-built structures from the as-designed values is dependent on various SLM processing parameters such as laser power, scanning speed and layer thickness (Hanzl et al., 2015). This leads to a variation in the expected and the obtained mechanical behavior of the cellular structures.

3.2 Tensile test

As mentioned in the previous section, FEM is carried out on as-designed structures and compared with the experimental stress-strain curve obtained from as-built structures. Due to the change in the porosity values after the manufacturing process, the mechanical properties of the samples are higher than the expected values (Amin Yavari et al., 2015; Cuadrado et al., 2017). The effect of porosity on the behavior of different topology values can be studied from the stress-strain curves shown in Fig. 2. Looking at the FEM results of the as-designed structures, regular structures have better stiffness and strength values as compared to the irregular and random structures for all the porosity values. An exception is seen in Fig.2(d) for the case of 1550 samples, this depends completely on the section of the random structure considered for the FE analysis. For 1520 samples which have highest porosity in both designed and as-built structure, the behavior of the irregular and random structure overlaps to a considerable extent. From Fig. 2(a), effect of cell topology has the least effect on samples with lowest porosity (0720) since the stress-strain curves of regular, irregular and random structures are very close.

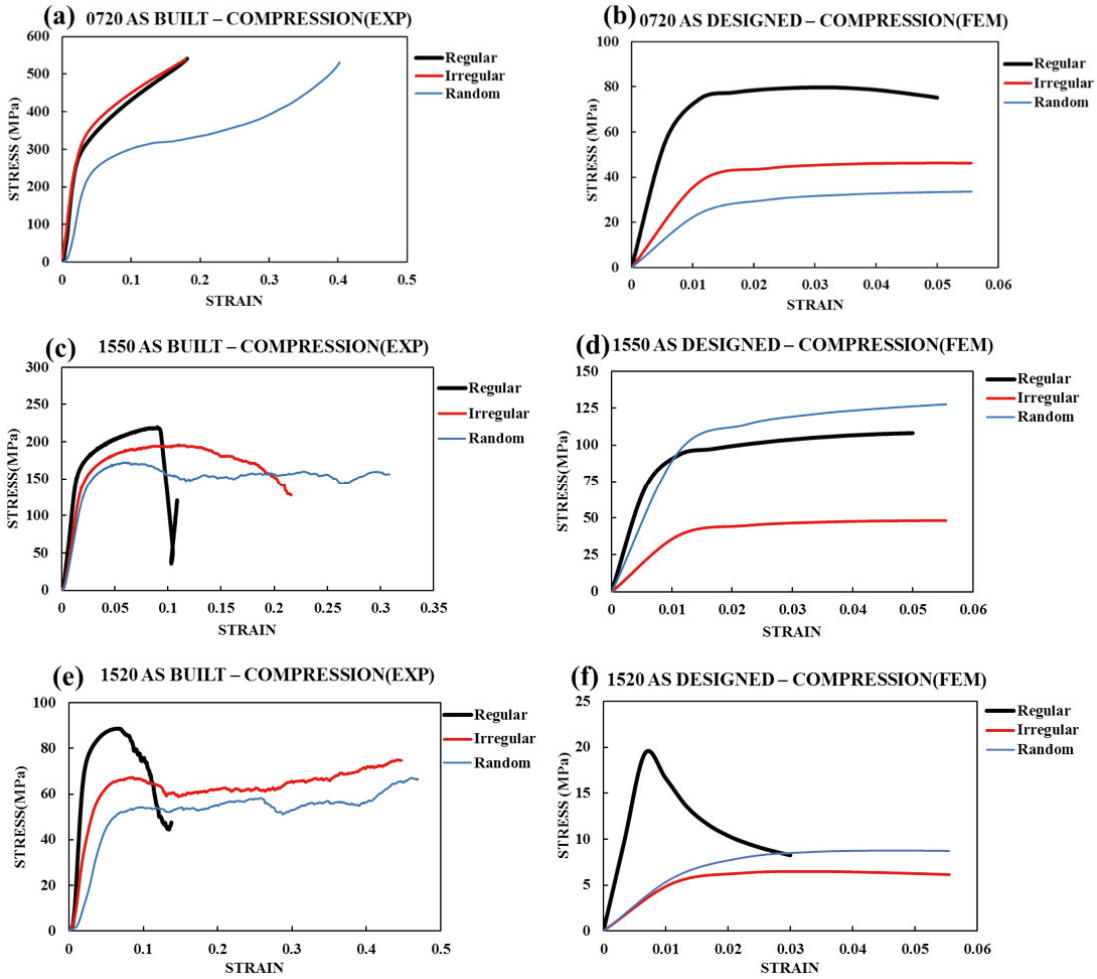

Fig. 3. Compression stress-strain curves in experimental and FEM: (a) and (b) 0720, (c) and (d)1550, (e) and (f) 1520

3.3 Compression Test

As discussed before, to initiate the compression phenomenon in the FE models, a small horizontal displacement is given along with the vertical displacement value. The stress-strain curves for all the samples in FEM and experimental

are as shown in Fig.3. As seen in tensile test results in previous section, a clear distinction between the different cell topology results is seen in the as-designed structures. From Fig.3(f) it is seen that the stress in the regular structure decreases as soon as the yielding starts, this is due to the buckling phenomenon that is predominant at high porosity values and with straight struts. As-built structures of 1550 and 1520 shown in Fig 3 (d) and (e) show a similar behavior, where stiffness and strength of the structure decreases with increase in the randomness of the structure. Irregular and random structures of 1520 and 1550 show a sustained plateau region after yielding due to the bending dominated behavior of the struts while compared to the regular structures. The behavior of the lowest porosity 0720 samples is like that seen in the tensile test, the stress in the specimen increase with increasing strain and no plateau region is observed for any of the cell topologies. The testing of the specimens had to be stopped before failure since the load exceeded the machine capacity of 100kN.

In our previous work, the stiffness and strength of these cellular structures under tensile and compression loads are discussed. A considerable decrease in Young's modulus under compression loading was observed when compared to tensile loading. To the investigate this, FEM of as-designed structures was carried out in both tensile and compression. No changes in the Young's modulus was seen for the as-built structure. Comparision of FE and experimental results of the as-built regular structures in tensile and compression are explained in the following section.

3.4 Comparision of experimental and finite element results of as-built regular structures.

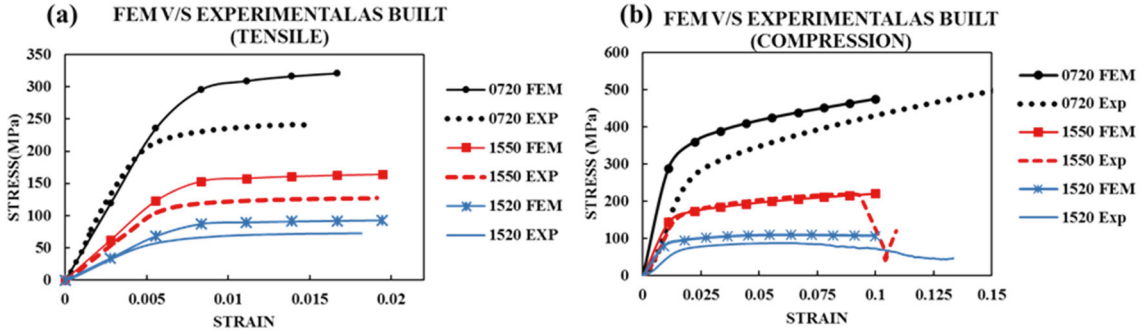

Fig. 4. Comparison of FEM and experimental behaviour of as-built regular structures (a) Tensile loading (b)Compression loading

The results comparing the experimental and the FE analysis for tensile test are as shown in Fig.4(a). Similar results are obtained for the compression behavior of cubic and diamond lattice with less than 18% error (Kadkhodapour et al., 2015), as discussed in the materials and methods section. It can be seen from the curves that the elastic region of the curves is near, thus the Young's modulus obtained from the FE modelling is within the variation range of the experimental values obtained. While analyzing the curve in beyond the elastic region, an early yielding is observed in the as-built printed samples when compared to the perfect FE model. Also, the ultimate tensile strength is greater by 26% in FE analysis in comparison with the experimental data. This difference in the plastic region can be attributed to the fact that defects such as strut waviness, internal defects, missing struts have not been considered in the FE model.

As mentioned before, for simulating the compression testing and to introduce buckling in the FE analysis a horizontal displacement of 0.1mm is applied for all the specimens. From Fig 4(b) the compression behavior of all the samples from experiments were replicated in the FE analysis as well. The curves of 1550 samples have a clear overlapping while a slight deviation in terms of the strength and stiffness values have been observed for 0720 and 1520 samples. A 20-25% difference is seen in strength and stiffness values of the 0720 and 1520 regular structures.

4.Conclusion

Cellular structures with three different topologies and under three different porosity values were manufactured using SLM. The samples were subjected to tensile and compressive loading. To understand the difference in the

behavior of the as-built and as-designed samples, finite element analysis was carried out on the as-designed and regular as-built structures. Following conclusions are drawn from the discussion in the previous section.

- Comparing the samples produced from SLM with the as-designed structures, an increased strut thickness is obtained. This increase in the thickness affects the mechanical properties and their behavior with respect to the topology.
- From the stress-strain behavior it is seen that, with increase in the porosity of the structures, effect of topology is clearly seen. The structures with the lowest porosity values showed least variation in the mechanical properties with increase in the randomness of the structure.
- In general, regular structures have higher strength and stiffness under all porosity ranges since the orientation of the struts are along the loading directions which is not the case for irregular and random configurations.
- In compression loading, the regular structures are susceptible to buckling phenomenon and the irregular and random structures are subjected to bending. Thus, regular structures are more suitable for structural applications, while irregular and random structures are suitable for applications with bending/compression loading since they exhibit a large and constant plateau region.
- The simulation results of the as-built regular structures indicate that, matching the porosity of the FE model and the printed samples can yield comparable results in the elastic region.
- In order to replicate the exact behavior of the structures, inclusion of defects such as strut waviness, missing struts and varying thickness play a major role. Since an early yielding is observed in the experiments when compared to the simulation curve.

Acknowledgements

This work is part of the FAMAC Research Project, co-sponsored by Eurocoating S.p.A. and Provincia Autonoma di Trento (Regional Public Authority).

References

Amin Yavari, S., Ahmadi, S. M., Wauthle, R., Pouran, B., Schrooten, J., Weinans, H., & Zadpoor, A. A. (2015). Relationship between unit cell type and porosity and the fatigue behavior of selective laser melted meta-biomaterials. Journal of the Mechanical Behavior of Biomedical Materials, 43, 91–100. https://doi.org/10.1016/j.jmbbm.2014.12.015

Bobbert, F. S. L., Lietaert, K., Eftekhari, A. A., Pouran, B., Ahmadi, S. M., Weinans, H., & Zadpoor, A. A. (2017). Additively manufactured metallic porous biomaterials based on minimal surfaces: A unique combination of topological, mechanical, and mass transport properties. Acta Biomaterialia, 53, 572–584. https://doi.org/10.1016/j.actbio.2017.02.024

Cuadrado, A., Yánez, A., Martel, O., Deviaene, S., & Monopoli, D. (2017). Influence of load orientation and of types of loads on the mechanical properties of porous Ti6Al4V biomaterials. Materials and Design, 135, 309–318. https://doi.org/10.1016/j.matdes.2017.09.045

Dallago, M., Winiarski, B., Zanini, F., Carmignato, S., & Benedetti, M. (2019). On the effect of geometrical imperfections and defects on the fatigue strength of cellular lattice structures additively manufactured via Selective Laser Melting. International Journal of Fatigue, 124(November 2018), 348–360. https://doi.org/10.1016/j.ijfatigue.2019.03.019

Hanzl, P., Zetek, M., Bakša, T., & Kroupa, T. (2015). The influence of processing parameters on the mechanical properties of SLM parts. Procedia Engineering, 100(January), 1405–1413. https://doi.org/10.1016/j.proeng.2015.01.510

Helou, M., Vongbunyong, S., & Kara, S. (2016). Finite Element Analysis and Validation of Cellular Structures. Procedia CIRP, 50, 94–99. https://doi.org/10.1016/j.procir.2016.05.018

ISO Standard, ISO 13314, 2011. Mechanical testing of metals – Ductility testing – Compression test for porous and cellular metals. International Organization of Standards, Switzerland. www.iso.org

Kadkhodapour, J., Montazerian, H., Darabi, A. C., Anaraki, A. P., Ahmadi, S. M., Zadpoor, A. A., & Schmauder, S. (2015). Failure mechanisms of additively manufactured porous biomaterials: Effects of porosity and type of unit cell. Journal of the Mechanical Behavior of Biomedical Materials, 50, 180–191. https://doi.org/10.1016/j.jmbbm.2015.06.012

Qiu, C., Yue, S., Adkins, N. J. E., Ward, M., Hassanin, H., Lee, P. D., … Attallah, M. M. (2015). Influence of processing conditions on strut structure and compressive properties of cellular lattice structures fabricated by selective laser melting. Materials Science and Engineering A, 628, 188–197. https://doi.org/10.1016/j.msea.2015.01.031

Raghavendra, S., Molinari, A., Fontanari, V., Luchin, V., Zappini, G., Benedetti, M., … Klarin, J. (2018). Tensile and compression properties of variously arranged porous Ti-6Al-4V additively manufactured structures via SLM. Procedia Structural Integrity, 13, 149–154. https://doi.org/10.1016/j.prostr.2018.12.025

Taniguchi, N., Fujibayashi, S., Takemoto, M., Sasaki, K., Otsuki, B., Nakamura, T., … Matsuda, S. (2016). Effect of pore size on bone ingrowth into porous titanium implants fabricated by additive manufacturing: An in vivo experiment. Materials Science and Engineering C, 59, 690–701. https://doi.org/10.1016/j.msec.2015.10.069

Yang, L. (2016). A study about size effects of 3D periodic cellular structures. Solid Freeform Fabrication 2016, 2181–2193.